2023 IEEE/ASME International Conference on Advanced Intelligent Mechatronics (AIM)
June 28-30, 2023. Seattle, Washington, USA

# Performance Comparison for Aggregation and Formation of Swarm Robots

Emre YAZICI
*Control & Automation Eng. Dept.*
*Istanbul Technical University, NISO Software Technologies*
Istanbul & Izmir, Turkey
yazici19@itu.edu.tr, yazicie@niso.com.tr

Prof. Dr. Hakan TEMELTAS
*Control & Automation Eng. Dept.*
*Istanbul Technical University*
Istanbul, Turkey
temeltash@itu.edu.tr

***Abstract*—In last few decades, the coordinated motion of swarm systems which consist of multiple autonomous robots are being intensively examined. These kinds of systems can have various functions such as the creation of the desired formation with physical or non-physical bondings, traveling to a desired position while maintaining the provided formation, and preventing collisions. Especially when looking at recent years, researchers have focused to potential function method to ensure the coordinated motion behavior of swarm systems. In this paper, two different potential function methods and controllers are selected and developed to provide collective behavior, integrated into a decentralized algorithm, implemented at the simulation level, and compared to present a useful guide for future developments on relevant topics. Potential function methods are evaluated and compared within the scope of swarm performance, which is investigated in three stages as gathering individuals, preventing the collisions, and deploying around the target. Thereafter, two different speed controllers are designed for each individual by using PID and sliding mode control methods. Moreover, evaluations of different sliding mode controllers are carried out by using combinations of 2 different sliding surfaces and 3 different switching functions, and the results are compared.**

***Index Terms*—swarm robotics, formation control, decentralized, PID, SMC, potential functions method, coordinated motion**

## I. Introduction

Nowadays, studies on a group of autonomous robots are essentially growing, and the types of research areas are vastly increased. From past to present, the researchers called these groups of robots under several different names such as multi-agent systems, Multi Robot Systems (MRS), and Swarm Robotics (SR). However, there are some distinct differences between SR and MRS [1]. The clarification of the differences between them is one of the significant initial steps before starting any types of study about SR. Multi-agent systems contain groups of agents that can perform tasks difficult for a single agent. There are three types of agents: active, passive, and variable [2]. MRS contains more than one individuals who are assigned identical or diversified tasks and can communicate each other [3]. The concept was first applied to robot arms in production lines by M.C. Maletz in 1983 [4]. The groups of same breed animals such as birds, fishes, wolves are called as swarm. These animals behave collectively for hunting, feeding, and also to protect themselves. M. Dorigo and E. Şahin indicated that all studies which contain groups of robots cannot be called SR, and specified several features to distinguish SR from the MRS such as containing many number of robots, being scalable, homogeneous, decentralized [1].

G. Beni has developed a decentralized system that contains multiple robots in 1988, and he called this system the cellular robotic which is mentioned previously by Fukuda [5]. Beyond this, he and his colleague, J. Wang, continued this study and presented their final works at a conference. However, A. Meystel imitated their study to a swarm more than cellular robots. After this idea, G. Beni and J. Wang have described swarm intelligence by looking at their studies on cellular robotics, and swarm robotics born [6].

Formation control algorithms are defined as centralized, decentralized, and hybrid. Centralized methods use one algorithm executed in a computer to control all individuals, while decentralized algorithms reuse one algorithm for each individual, allowing them to behave independently. However, decentralized algorithms are more complex and have higher error tolerances than centralized ones. Combining centralized and decentralized methods is called hybrid. [7]. Recent decentralized coordinated motion studies mainly use the potential functions method due to its effectiveness and simple implementation in dynamic environments [8-14]. A. R. Merheb, R. Ghamrawi, and A. Eid used Potential Functions (PF) and Sliding Mode Control (SMC) to develop a formation creation algorithm for a firefighting scenario using two-wheeled nonholonomic vehicles as individuals to provide emergent swarm behavior [8]. X. Fu, H. Wang, J. Pan and X. Gao improved the PF method for unmanned aerial vehicles by using basic graph theory to derive relationships between individuals and defining a virtual leader to achieve and maintain the desired formation [9]. Also, they studied obstacle avoidance, formation maintenance, and reconstruction by using the artificial potential field method [10]. Lately, B. Gh. Elkilany, A. A. Abouelsoud, A. M. R. Fathelbab and H. Ishii produced the artificial neural network to optimize the potential force parameters, thus the robot swarm could travel without oscillation in narrow spaces between obstacles [11]. They also proposed another method to obtain the potential force parameters called fuzzy inference tuning. This method was improved to tune the potential force gain parameters with the relation of member's status [12].

978-1-6654-7633-1/23/$31.00 ©2023 IEEE

This paper makes a contribution to the field of swarm robotics by providing a comprehensive guide for the development of potential function methods and speed controllers for aggregation and formation problems. To achieve this, the study compares and contrasts two accepted potential function methods and analyzes their advantages and limitations. Additionally, two commonly used speed controller methods, namely PID and SMC, are designed, evaluated, and compared. The findings of this study provide valuable insights and practical recommendations for researchers and practitioners working in the field of swarm robotics.

The content of this paper is organized as follows. Section II describes the motivation and problem formulation of the swarm robot's formation and maintenance. Section III presents the selected potential function methods. Section IV proposes the speed controllers and comparison. Section V contains the simulation results. Finally, Section VI exhibits the results.

## II. Motivation and Problem Definition

### A. Motivation

The works in the field of SR possess significant results since the emergent aims start to denote critical duties such as the search&rescue (in other words disaster response) robotics applications, defense, and mars missions. For instance, the autonomous formation creation by swarm robots is one of the biggest problems for mars missions to create the colony. Shortly, it can be said that these duties are essential for people's lives and future. Thus, studying in this field is one of the inalienable motivations for researchers.

### B. Problem Definition

In this paper, the problems of formation creation and maintenance during motion of swarm robots are considered. In order to provide more accurate and similar results to real-world applications, the same scenario is applied for all methods, and it is assumed to have non-linear friction for each individual. Thus, the kinematic model of individuals can be derived by using Newton's second law as:

$$\dot{\vec{v}}_i = \frac{\vec{u}_i - k\vec{v}_i}{m}, \tag{1}$$

where k denotes non-linear friction gain, and m is the strictly positive mass of an individual. First of all, r defines the number of individuals in the swarm, and the positions of individuals are denoted by $p_i$ where $i \in 1:r$. Moreover, swarm robots are expected to travel from their initial positions, which are denoted by $p_i^0$ where $i \in 1:r$, to the target with forming a triangular shape and without any collision between each other and with an obstacle. The initial positions of individuals, and the positions of point obstacle ($p_o$) and target ($p_t$) are selected as in Fig. 1. Evaluations are made for the swarm performance which is divided into three different sub-behaviors as the aggregation, formation, and coordinated motion. Moreover, swarm performance can also be examined under three different phases according to the defined behaviors such as gathering, obstacle avoidance, and deployment.

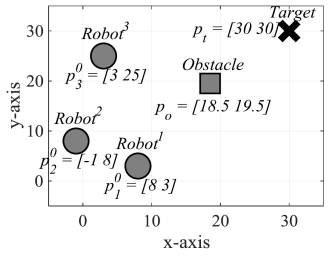


Fig. 1. The initial positions of three individuals and specified positions of target and obstacle in the scenario.

The swarm robots are assumed to be in the gathering phase from the beginning until all distances between every two individuals stay between desired distance with $\pm$ 0.1m precision for 0.01s. The end time of the gathering phase is also defined as gathering time. After the gathering phase, the swarm robots start traveling to the target while maintaining their formation. In the case of one individual is affected by repulsive force due to penetration of the repelling region, the obstacle avoidance phase starts. Similarly, this phase ends when all individuals escape from the effect of repulsive force. Lastly, deployment phase starts when an individual across the target with the desired distance between target and individual. Since swarm robots are assumed to form a triangular shape around the target, the distance between an individual and target can be calculated by simple geometry. So, the individuals are assumed to reach a position where their distances between the target are 2.88m.

## III. Potential Function Methods

### A. The First Key Study

The attraction force, $f^1_{att_i}$, is formulated as:

$$f^1_{att_i}(\vec{p}_i, \vec{p}_t) = -\beta(\vec{p}_i - \vec{p}_t), \tag{2}$$

where $\vec{p}_i$ and $\vec{p}_t$ represent position vectors of the $i^{th}$ individual and target, respectively. Moreover, the attractive force gain is implemented and shown with $\beta$ [8]. The repulsive force, $f^1_{rep_i}$, that keeps the individuals in a safe region and avoid them to crash with the obstacle is derived as:

$$\xi_o = \|\vec{p}_i - \vec{p}_o\|, \tag{3}$$

$$f^1_{rep_i}(\vec{p}_i, \vec{p}_o) = -\alpha e^{-\frac{\xi_o^2}{c}} \times \frac{2}{c} \times (\xi_o^2 - 1), \tag{4}$$

where $\vec{p}_o$ represents obstacle position vector, and $\|.\|$ denotes the vector norm. Moreover, $\alpha$ and c are used as gains of the repulsive force [8]. The interactive force, $f^1_{int_i}$, is derived as:

$$\xi_j = \|\vec{p}_i - \vec{p}_j\|, \tag{5}$$

$$f^1_{int_i}(\vec{p}_i, \vec{p}_j) = (a_{ij} + b_{ij}e^{-\xi_j^2}) \times \frac{2}{c_{ij}} \times (\xi_j^2 - 1), \tag{6}$$

where $\vec{p}_j$ represents position vector of $j^{th}$ neighbor. $a_{ij}$, $b_{ij}$ and $c_{ij}$ are the interactive force gains which have a relationship

with the desired distance ($d_{des_{ij}}$) between $i^{th}$ individual and $j^{th}$ neighbor which also provides the swarm to form the triangular shape with $d_{des_{ij}}$ side lengths as:

$$a_{ij} = b_{ij} \times e^{-\frac{d^2_{des_{ij}}}{c_{ij}}}. \tag{7}$$

Eventually, the swarm robots are supposed to achieve desired swarm behaviors by using $f^1_{total_i}$ which is the summation of three forces [8].

### B. The Second Key Study

The attraction force, $f^2_{att_i}$, is formulated as:

$$f^2_{att_i}(\vec{p}_i, \vec{p}_t) = \begin{cases} \frac{-(\vec{p}_i - \vec{p}_t)}{d_{lim_t}}, & d^i_t < d_{lim_t} \\ \frac{-(\vec{p}_i - \vec{p}_t)}{d^i_t}, & \text{otherwise} \end{cases}, \tag{8}$$

where distance between $i^{th}$ individual and target is expressed with $d^i_t$. $f^2_{rep_i}$ that keeps the individuals in safe region and avoid them to crash with the obstacle is derived as:

$$\xi_{rep} = \frac{1}{(d^i_o)^2} \times \left(\frac{1}{d^i_o} - \frac{1}{d_{lim_o}}\right) - (d^i_o - d_{lim_o}), \tag{9}$$

$$f^2_{rep_i}(\vec{p}_i, \vec{p}_o) = \xi_{rep} \times \vec{u}_{p_{i-o}}, \tag{10}$$

where distance between $i^{th}$ individual and obstacle is expressed with $d^i_o$, and the limit distance to detect obstacle is denoted by $d_{lim_o}$. The unit vector between the $i^{th}$ individual and obstacle is represented with $\vec{u}_{p_{i-o}}$ [11]. $f^2_{int_i}$ is derived as:

$$\xi_{int} = \frac{1}{(d_{ij})^2} \times \left(\frac{1}{d_{ij}} - \frac{1}{d_{des_{ij}}}\right) - (d_{ij} - d_{des_{ij}}), \tag{11}$$

$$f^2_{int_i}(\vec{p}_i, \vec{p}_j) = \begin{cases} \xi_{int} \times \vec{u}_{p_{i-j}}, & d_{ij} < d_{des_{ij}} \\ \frac{-(\vec{p}_i - \vec{p}_j)}{d_{ij}}, & \text{otherwise} \end{cases}, \tag{12}$$

where $d_{ij}$ denotes the distance between $i^{th}$ and $j^{th}$ individuals. The unit vector between these individuals is presented with $\vec{u}_{p_{i-j}}$. Eventually, the swarm robots are supposed to achieve desired swarm behaviors by using $f^2_{total_i}$ which is the summation of three forces [11].

## IV. Speed Controller Design

In this paper, we propose the design of two distinct speed controllers, namely PID and SMC, which represent linear and non-linear methodologies, respectively. These control methods have been chosen due to their well-established and widely adopted architectures in the field. Speed controllers are designed according to three criteria to obtain similar performances. These criteria are chosen via different studies about the real-applications such as driving of motors, controlling of robots to design applicable speed controllers [15-18].

***Criteria I:*** The settling time must be less than 1.5 seconds.

***Criteria II:*** The overshoot of must be less than %4.

***Criteria III:*** The rise time of must be less than 1 second.

Some additional assumptions are involved to be able to generate reasonable results.

***Assumption I:*** The nonlinear friction force gain, k, is selected as $\frac{\vec{v}_i}{100}$ to provide higher friction force in higher velocities (thus "$\vec{v}^2_i$" term appears in (1) which brings nonlinearity), and m is assumed to be unity.

***Assumption II:*** The speed controller generates the force that will be applied to the individual according to the error of reference and actual velocities. However, the individuals cannot support the motion under unlimited force. So, the speed controller's output is saturated to 15 N. The velocities of the individuals are also limited to 25 m/s for similar purposes.

### A. PID Speed Controller

PID control is one of the feedback control methods which is needed to calculate error value continuously. Since it is a commonly used and well-known control method, it is first chosen to control the applied force of the individuals [15,16]. The control input which is equal to applied force to each individual can be computed by using PID controller as:

$$\vec{u}_{PID_i} = K_p \vec{e}_i + K_i \int \vec{e}_i dt + K_d \frac{d\vec{e}_i}{dt}, \tag{13}$$

where $K_p$, $K_i$ and $K_d$ are the positive proportional, integral, and derivative gains, respectively. $\vec{e}_i$ denotes the velocity error, $(\vec{v}_{ref_i} - \vec{v}_i)$, where $\vec{v}_{ref_i}$ is the reference velocity of $i^{th}$ individual. The controller type can be selected as P, PI, PD, PID depending on the presence of parameters [19,20]. Parameters are manually tuned for speed controller of individuals to provide given criteria. The characteristic of step responses for different parameters are determined as in Table I.

Tuning process is started with the first set, P-type, given in Table I. However, the friction force causes the steady-state error. Thus, the settling time and overshoot cannot be measured and it is specified as Not a Number (NaN). Despite this, the rise time is obtained as 0.24s. To get rid of the friction effect, integral component is added, PI-type. However, the overshoot increased due to the summation of velocity errors in time. Then, proportional constant is increased as in third set in Table I. Thus, the overshoot is damped according to results of the second set. So, the settling and rise time results are obtained way better. Lastly, the derivative component is added to provide a better damping effect on controlling the system as in the fourth set, and the settling time decreased. Thus all criteria are achieved with the fourth set, PID-type, in the Table I.

TABLE I
STEP RESPONSES FOR DIFFERENT PID PARAMETERS.

| **PID Parameters** | | | **Step Response Characteristics** | | |
|---|---|---|---|---|---|
| $K_p$ | $K_i$ | $K_d$ | **Settling Time (s)** | **Overshoot (%)** | **Rise Time (s)** |
| 8 | 0 | 0 | NaN | NaN | 0.24 |
| 2 | 5 | 0 | 2.30 | 7.74 | 0.53 |
| 8 | 5 | 0 | 1.31 | 0 | 0.29 |
| 8 | 5 | 0.5 | 0.76 | 0 | 0.39 |

### B. SMC Speed Controller

SMC is a non-linear control method that forces the systems to reach and stay on a specified sliding surface ($S_i^t$ where t denotes the enumeration of used sliding surface). The SMC control input ($\vec{u}^t_{SMC_i^b}$ where b represents the enumeration of used switching function) is derived according to this sliding surface and the mathematical model of the system [21]. The control input contains two different variables, equivalent and switching. The equivalent effect can be obtained while zeroing the derivative of the sliding surface since it contains the $\vec{u}^t_{SMC_i^b}$, and this drives the system to the sliding surface from its starting point in the model space. Moreover, the other effect is to force the system to stay on the sliding surface during its motion which is the switching effect [22,23]. However, this also causes one of the biggest problems of SMC which is chattering [22].

In this thesis, two different sliding surfaces are used individually for SMC speed controller of each individual to find the most suitable ones. The sliding surfaces are chosen as:

$$S_i^1 = \left(\frac{d}{dt} + \gamma\right)^{n-1} \vec{e}_i, \tag{14}$$

$$S_i^2 = \left(\frac{d}{dt} + \gamma\right)^{n} \int \vec{e}_i, \tag{15}$$

where n denotes the degree of the individual's plant, and $\gamma$ is strictly constant [21,24]. The equivalent parts regarding to the selected sliding surfaces are derived as:

$$\vec{u}^{eq_1}_{SMC_i} = m\dot{\vec{v}}_{ref_i} + 0.01\vec{v}_i\vec{v}_i, \tag{16}$$

$$\vec{u}^{eq_2}_{SMC_i} = -\gamma m\left(\vec{v}_i - \vec{v}_{ref_i}\right) + m\dot{\vec{v}}_{ref_i} + 0.01\vec{v}_i\vec{v}_i. \tag{17}$$

Furthermore, the switching function is firstly selected as:

$$\vec{u}^t_{sw_i^t} = -k^1_{sw_1} sign(S_i^1), \tag{18}$$

where $k^t_{sw_b} \forall (t,b)$ are strictly constant [22]. SMC behavior which is the reaching and sliding phases can be examined in the phase portrait of sliding surfaces as in Fig. 2. The chattering is traced in the sliding surfaces for both $\vec{u}^1_{SMC_i^1}$ and $\vec{u}^2_{SMC_i^1}$. To get rid of the chattering problem, other switching functions are implemented and analyzed as:

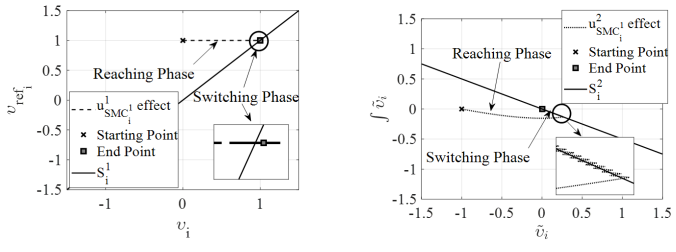


(a) (b)

Fig. 2. Phase portrait of sliding surfaces and individual's behaviours with (a) the first, (b) the second sliding surfaces via the first switching function.

$$\vec{u}^t_{sw_i^2} = -k^1_{sw_2} tanh(S_i^1), \tag{19}$$

$$\vec{u}^t_{sw_i^3} = -k^1_{sw_3} \frac{S_i^1}{|S_i^1| - \Omega}, \tag{20}$$

where $\Omega$ are strictly constant [24, 25]. All switching functions can be plotted as in Fig. 3 by selecting the different $\Omega$ in (20), and can be seen that all saturate to the selected $k^t_{sw_b}$ constant value which is 2. However, the smoothness of the functions can vary. It is crucial to note that having excessively smooth functions can result in reduced sensitivity and compromise the robustness of the SMC method. $\vec{u}^1_{sw_i^3}$ provides the most smooth result, but decreasing the value of $\Omega$ increases the quickness of the response. The characteristic of step responses for combinations of sliding surfaces and switching functions are determined as in Table II. The results in Table II show that there is only one option to ensure the given speed controller criteria. This option is the $\vec{u}^1_{SMC_i^3}$ where $\Omega$ is equal to 0.5 for the $\vec{u}^1_{sw_i^3}$. Eventually, $\vec{u}^1_{SMC_i^3}$ with $k^1_{sw_3}$ is designed as:

$$\vec{u}^1_{SMC_i^3} = m\dot{\vec{v}}_{ref_i} + 0.01\vec{v}_i\vec{v}_i - 2\frac{\vec{e}_i}{|\vec{e}_i| + 0.5}. \tag{21}$$

The stability of control input for reaching phase is proved by applying the Lyapunov's second stability theorem as:

$$\frac{1}{2}\frac{d}{dt}(S_i^1)^2 = S_i^1 \dot{S}_i^1 \leq -\eta_1 |S_i^1|. \tag{22}$$

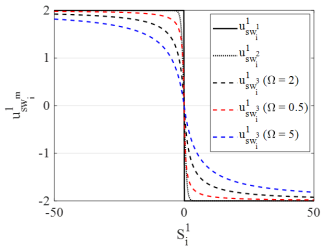


Fig. 3. The possible values of three different switching functions by using the first sliding surface.

TABLE II
STEP RESPONSES FOR DIFFERENT SMC PARAMETERS.

| SMC Types | Ω | Step Response Characteristics | | |
|---|---|---|---|---|
| | | Settling Time (s) | Overshoot (%) | Rise Time (s) |
| $\vec{u}^1_{SMC_i^2}$ | - | 2.03 | 0 | 1.16 |
| $\vec{u}^2_{SMC_i^2}$ | - | 2.78 | 14.65 | 0.39 |
| $\vec{u}^1_{SMC_i^3}$ | 2 | 4.39 | 0 | 2.59 |
| $\vec{u}^2_{SMC_i^3}$ | 2 | 1.46 | 12.74 | 0.57 |
| $\vec{u}^1_{SMC_i^3}$ | 0.5 | 1.46 | 0 | 0.95 |
| $\vec{u}^2_{SMC_i^3}$ | 0.5 | 2.49 | 18.06 | 0.39 |
| $\vec{u}^1_{SMC_i^3}$ | 5 | 9.91 | 0 | 5.82 |
| $\vec{u}^2_{SMC_i^3}$ | 2 | 6.60 | 8.53 | 0.72 |

Let's simplify $S_i^1$ by taking $\vec{u}_{SMC_i}^{eq_1}$ as $\vec{u}_{SMC_i^3}^1$.

$$k_{sw_3}^1 \leq \frac{\eta_1}{\left|\frac{S_i^1}{|S_i^1|+\Omega}\right|}, \forall S_i^1 \in R \notin 0. \tag{23}$$

The derived control input is ensured to provide stable results, and also force the sliding surface to be zero, since $k_{sw_3}^1$ is selected while ensuring the equations in (23).

### C. Speed Controllers Performance Comparison

Designed PID and SMC speed controllers are evaluated by integrating with the second key study. The swarm performance is obtained as in the Table III.

## V. Simulation

$f_{total_i}^1$ and $f_{total_i}^2$ are applied for each individual, and scenario is simulated, respectively. The distances between individuals-target, individuals-obstacle, and individual-individual are shown in Fig. 4 and Fig. 5. Moreover, the algorithms are also tested for different number of obstacles and initial positions as in Fig. 6.

TABLE III
Swarm Performance For PID and SMC.

| Performance Parameter | PID | SMC |
|---|---|---|
| Aggregation Time | 6.31s | 8.86s |
| Obstacle Avoidance Phase Start Time | 11.38s | 12.13s |
| Obstacle Avoidance Phase End Time | 27.22s | 27.65s |
| Deployment Phase Start Time | 32.54s | 33.13s |
| Deployment Phase End Time | 55.94s | 56.33s |
| Final distance between individuals and target ($d_t^i \forall i$) | 2.72m | 2.72m |
| Final distance between individuals ($d_i j \forall i$) | 4.69m | 4.69m |

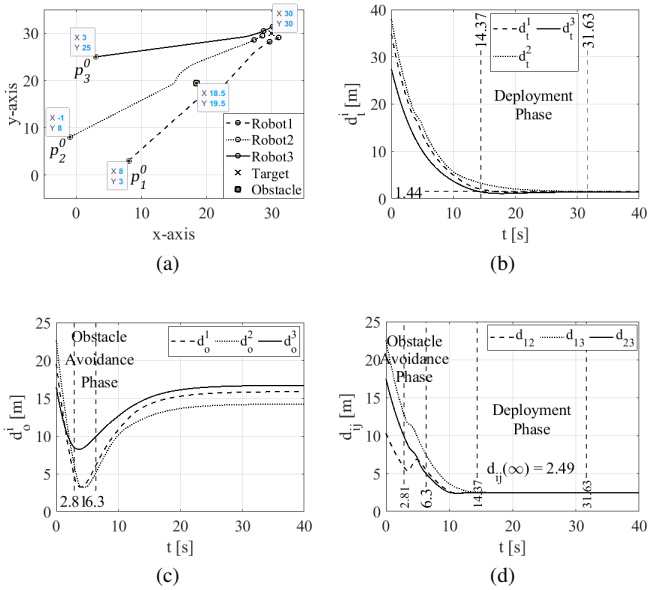


Fig. 4. (a) The swarm motion, distances between (b) robot-target, (c) robot-obstacle, and (d) robot-robot by using PF of the first key study.

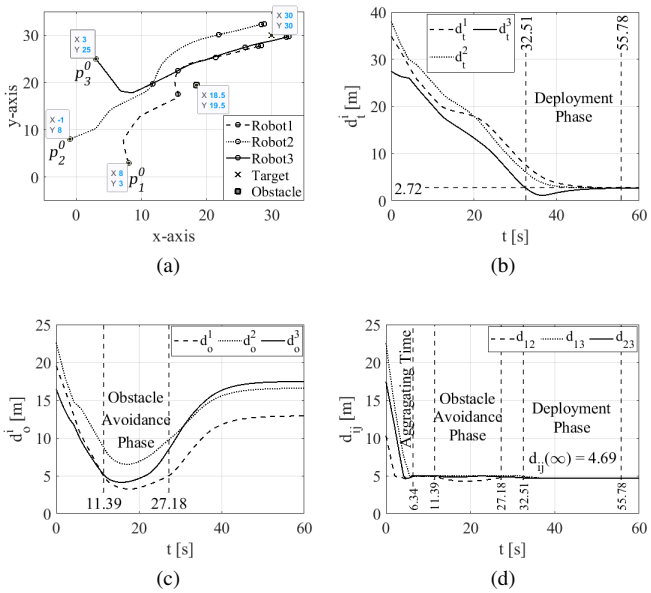


Fig. 5. (a) The swarm motion, distances between (b) robot-target, (c) robot-obstacle, and (d) robot-robot by using PF of the second key study.

## VI. Discussion And Results

Results are evaluated for scalability and swarm performance. The swarm formation is provided by using the interactive PF for both key studies, and it can be seen that interactive PF depend on the position of individuals and the distances between them. In this paper, the desired distances between each individual are assumed to be equal. So, the number of individuals are limited to three. To increase the number of robots in the swarm, some necessary additions/configurations should be performed such as changing of the interactive PF according to the total number of individuals and implementation of a graph which contains different desired distances for each size of the swarm. The applied and evaluated key studies are suitable for increasing the number of individuals by means of decentralized implementation. Thus, it can be interpreted that the key studies can be used for swarms with higher number of robots with integrating one adaptive selection for desired distances between individuals. The aggregation and formation

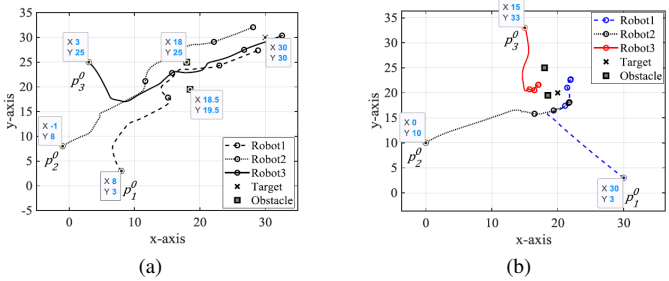


Fig. 6. The swarm motion with different (a) number of obstacles, and (b) initial positions.

behaviors of swarm robots are provided for the second key study as seen in Fig. 5. However, it has not been obtained in the first key study as in Fig. 4 due to the absorption of interactive effects by the other forces. In other words, the first key study has the lack of target and obstacle detecting ranges which inhibit the aggregation and formation performance. The coordinated motion is provided for both methods, since the swarm robots can reach the target without any collision with each other and obstacle. However, the desired distances in Fig. 4b and Fig. 4d are obtained as 1.44m for $d_t^i \forall i$ and 2.49m for $d_{ij} \forall i$ where $i \neq j$ for the first key study. Beyond, they are obtained as 2.72m for $d_t^i \forall i$ and 4.69m for $d_{ij} \forall i$ where $i \neq j$ for the second key study as in Fig. 5b and Fig. 5d while the desired distances are given as 2.88m for $d_{des_t}$, and 5m for $d_{des_{ij}}$. So, it can be concluded that the first key study fails to achieve the desired formation with the specified distances between individuals. In contrast, the second key study successfully accomplishes the desired deployment around the target.

PID and SMC speed controllers in Section IV are evaluated with the same scenario and second key study. The results are obtained as in Table III. The aggregation behavior of swarm robots is achieved more faster by using PID speed controller. While the obstacle avoidance duration can be calculated as 15.84s for PID and 15.52s for SMC, the deployment phase duration can be found as 23.40s for PID and 23.20s for SMC. These results show that SMC provides faster responses for obstacle avoidance and deployment phases. Lastly, PID and SMC speed controllers can be evaluated to provide similar performances for the final situation for the desired distances between individual-target and individual-individual with 0.16m and 0.31m errors, respectively.

To sum up, swarm performance is provided way better for the second key study due to its successful aggregation and formation abilities. On the other hand, the first key study offers coordinated motion with sensitive collision avoidance performance. However, its reliability and feasibility are worse than the second key study due to its lack of detecting range ability, and the desired deployment around the target cannot be also achieved. Furthermore, both PID and SMC speed controllers are evaluated to provide similar and successful performances. However, it should not be ignored that the models of individuals are generally non-linear for real applications. So, one of the non-linear based control approaches is supposed to provide better results in all conditions. When it is looked to the step responses of PID in Table I, there is an unstable condition. On the other side of coin, SMC control method provides stable results. Finally, SMC can be ensured as more suitable control method for swarm robotic applications.

## ACKNOWLEDGMENT

Special thanks to NISO Software Technologies, ASELSAN and Istanbul Technical University for their endless supports and opportunities.

## REFERENCES

[1] M. Dorigo and E. Şahin (2004). Guest editorial: Swarm robotics, Autonomous Robotics, 17(2-3), 111-113.
[2] Y. Kubera, P. Mathieu and S. Picault (2010). Everything can be Agent!.
[3] Y. Cai and S.X. Yang (2012). A Survey on Multi-Robot Systems, World Automation Congress, 1-6.
[4] M.C. Maletz (1983). Production Systems For Multi-Robot Control A Tutorial, IEEE Workshop on Languages for Automation, Chicago, USA.
[5] G. Beni (1988). The Concept Of Cellular Robotic System, IEEE International Symposium on Intelligent Control 1988, 57-62.
[6] G. Beni and J. Yang (1993). Swarm Intelligence in Cellular Robotic Systems, Robots and biological systems: towards a new bionics?, 703-712.
[7] K. Kiattisin (2016). Formation Control of Mobile Robots: Survey.
[8] A. R. Merheb, R. Ghamrawi and A. Eid (2018). Navigation and Formation Control of a Tracked Robot Swarm for Firefighting Missions, 2018 IEEE International Multidisciplinary Conference on Engineering Technology (IMCET), IEEE, 1-6.
[9] X. Fu, H. Wang, J. Pan and X. Gao (2019). A Distributed Formation Control Method of Swarm UAVs Based on Artificial Potential Field and Consensus Strategy, 2019 Australian & New Zealand Control Conference (ANZCC), 210-214.
[10] X. Fu, J. Pan, H. Wang and X. Gao (2020). A formation maintenance and reconstruction method of UAV swarm based on distributed control, Aerospace Science and Technology.
[11] B.G. Elkilany, A.A. Abouelsoud, A.M.R. Fathelbab and H. Ishii (2020). A proposed decentralized formation control algorithm for robot swarm based on an optimized potential field method, NEURAL COMPUTING & APPLICATIONS.
[12] B.G. Elkilany, A.A. Abouelsoud, A.M.R. Fathelbab and H. Ishii (2020). Potential Field Method Parameters Tuning Using Fuzzy Inference System for Adaptive Formation Control of Multi-Mobile Robots, Robotics, 9(1).
[13] B. Bao (2023). Research on real-time path planning and obstacle avoiding for mobile robot swarms based on an advanced artificial potential field method, IEEE 2nd International Conference on Electrical Engineering, Big Data and Algorithms, 1747-1752.
[14] Wu, W., Qin, X., Qin, J., Yu, X., and Liu, Q. (2023). Flexible Formation Control of Multiple Unmanned Vehicles Based on Artificial Potential Field Method, In Bio-Inspired Computing: Theories and Applications: 17th International Conference, 567-577.
[15] C. C. Hang, K. J. Astrom and W. K. Ho (1991). Refinements of the Ziegler-Nichols tuning formula, In IEE Proceedings D (Control Theory and Applications), Vol. 138, No. 2, 111-118.
[16] W. M. Lee and H. P. Huang (1996). Stabilization of nonholonomic mobile robots by a GA-based fuzzy sliding mode control, Soft Computing in Intelligent Systems and Information Processing. Proceedings of the 1996 Asian Fuzzy Systems Symposium, IEEE, 388-393.
[17] R. M. Mansilla, D. Chaos, J. Aranda and J. M. Diaz (2012). Application of quantitative feedback theory techniques for the control of a nonholonomic underactuated hovercraft, IET Control Theory & Applications, 6(14), 2188-2197.
[18] B. D. Argo, Y. Hendrawan, D. F. Al Riza and A. N. J. Laksona (2015). Optimization of PID controller parameters on flow rate control system using multiple effect evaporator particle swarm optimization, International Journal on Advanced Science, Engineering and Information Technology, 5(2), 6-12.
[19] K. H. Ang, G. Chong and Y. Li (2005). PID control system analysis, design, and technology, IEEE transactions on control systems technology, 13(4), 559-576.
[20] K. J. Aström, K. Johan and T. Hagglund (2001). The future of PID control, Control engineering practive, 9(11), 1163-1175.
[21] J. J. E. Slotine and W. Li (1991). Applied nonlinear control, Vol.199, No.1, Englewood Cliffs, NJ: Prentice hall.
[22] V. Utkin, J. Fuldner and J. Shi (1999). Sliding mode control in electromechanical systems, Vol.34, CRC press.
[23] V. Utkin and I. Vadim (2004). Sliding mode control Variable Structure Systems, from Principles To Implementation, 66.
[24] M. Furat and E. İlyas (2012). Experimental evaluation of sliding-mode control techniques, Çukurova Üniversitesi Mühendislik-Mimarlık Fakültesi Dergisi, 27(1), 23-37.
[25] C. Edwards and S. Spurgeon (1998). Sliding mode control: theory and applications, CRC Press.